A density functional theory for vapor-liquid interfaces using the PCP-SAFT equation of state

Joachim Gross[a)]

Engineering Thermodynamics, Process, and Energy Department, Delft University of Technology, 2628 CA Delft, The Netherlands

A Helmholtz energy functional for inhomogeneous fluid phases based on the perturbed-chain polar statistical associating fluid theory (PCP-SAFT) equation of state is proposed. The model is supplemented with a capillary wave contribution to the surface tension to account for long-wavelength fluctuations of a vapor-liquid interface. The functional for the dispersive attraction is based on a nonlocal perturbation theory for chain fluids and the difference of the perturbation theory to the dispersion term of the PCP-SAFT equation of state is treated with a local density approximation. This approach suggested by Gloor *et al.* [Fluid Phase Equilib. **194**, 521 (2002)] leads to full compatibility with the PCP-SAFT equation of state. Several levels of approximation are compared for the nonlocal functional of the dispersive attractions. A first-order non-mean-field description is found to be superior to a mean-field treatment, whereas the inclusion of a second-order perturbation term does not contribute significantly to the results. The proposed functional gives excellent results for the surface tension of nonpolar or only moderately polar fluids, such as alkanes, aromatic substances, ethers, and ethanoates. A local density approximation for the polar interactions is sufficient for carbon dioxide as a strongly quadrupolar compound. The surface tension of acetone, as an archetype dipolar fluid, is overestimated, suggesting that a nonisotropic orientational distribution function across an interface should for strong dipolar substances be accounted for. © *2009 American Institute of Physics*. [doi:10.1063/1.3263124]

I. INTRODUCTION

Interfaces play a determining role in the design of nanostructured materials and processes. The control and modification of interfacial properties and the resulting macroscopic behavior requires predictive models that are based on molecular theories. The most versatile and successful approach to describe interfaces is the classical density functional theory (DFT) for molecular fluids.[1] Prominent introductions to the DFT are due to Evans[2] and Davis,[3] and comprehensive reviews on recent advances and applications are available by Wu[4,5] and by Löwen.[6]

Equations of state derived from molecular theories are now routinely applied in engineering practice. They are parametrized for a wide variety of substances and mixtures and it is desirable to extend their applicability to interfacial properties. A successful theoretical framework for nonspherical and associating fluids, the statistical associating fluid theory (SAFT) equation of state, has been developed by Chapman *et al.*[7,8] based on Wertheim's thermodynamic perturbation theory of first order (TPT1).[9–12] Several modifications were suggested over the years,[13–17] with widespread applications.[18]

The TPT1 of Wertheim is formulated in density functional form and has been applied to inhomogeneous associating fluids in several studies.[19–25] In the molecular model of SAFT-type equations of state, one represents molecules as connected spherical segments, resembling the molecular con-

figuration of real molecules in a coarse-grained way. The connection of segments to form segment chains is achieved by considering a mixture of initially free spheres (with association sites) in the limit of complete association. The picture of initially free spheres that are connected to form chains leads to a very convenient ideal-gas reference. Free spheres serve as an ideal gas reference in this concept, whereas the ideal-gas contribution of multisegmented fluids would otherwise be determined by internal degrees of freedom and intramolecular energies.[26,27] Helmholtz energy functionals for the chain formation have been developed over many years[28–34] and accurate expressions have recently been proposed by Tripathi and Chapman.[26,27] Combined with the modified fundamental measure theory (FMT) for the hard-sphere system,[35–38] these expressions were shown to compare excellent with molecular simulation data.[26,39] The resulting Helmholtz energy functional of the hard-sphere reference fluid and the chain contribution as well as the association contribution simplify to the appropriate expressions in bulk-phase SAFT equations of state in the limit of homogeneous phases.

The dispersion term of many of the SAFT equations of state broadly applied in engineering context are not formulated in density functional form, because it would generally require a local resolution of the fluid structure and thus too high computational cost for the routine purpose of bulk phases. Gloor *et al.*,[40–42] however, proposed a prescription to consistently apply the DFT with these bulk-phase equations of state. It was shown that a DFT treatment of the dispersive

---

a)Electronic mail: j.gross@tudelft.nl.

131, 204705-1

attraction can be established based on perturbation theory, while any (small) difference between this dispersion term and the dispersion term of the engineering equation of state can with sufficient accuracy be described with a local density approximation (LDA). This allows for empirically parametrized models of bulk phases or higher-order perturbation theories to be combined with relatively simple density functional perturbation terms.

In this study the PCP-SAFT equation of state is employed with the approach of Gloor *et al.* Several levels of approximation are thereby evaluated: results of first- and second-order non-mean-field perturbation theories for chain fluids are compared to a mean-field approach. The contribution of capillary waves to the surface tension is estimated with a simple model that constitutes a first-order expansion of universal critical scaling behavior. The proposed Helmholtz energy functional is first applied to nonpolar and weakly polar substances and is then tested for strong dipolar and quadrupolar components.

II. MOLECULAR MODEL AND BULK EQUATION OF STATE

In SAFT-type equations of state one usually assumes molecules to be composed of chains of tangentially bonded spherical segments. The molecular model gives a coarse-grained representation of real molecules, where the detailed segment-configuration of a chain is not resolved. A segment is characterized by an interaction potential, in our case of Lennard-Jones type. The Lennard-Jones potential $u(r) = u_0(r) + u^{PT}(r)$ is decomposed into a repulsive part,

$$u_0(r) = 4\varepsilon[(\sigma/r)^{12} - (\sigma/r)^6]\Theta(\sigma - r), \tag{1}$$

and an attractive part,

$$u^{PT}(r) = 4\varepsilon[(\sigma/r)^{12} - (\sigma/r)^6]\Theta(r - \sigma), \tag{2}$$

with Θ as the Heaviside step function. The fluid with the repulsive part of the segment interaction potential is described as a hard-sphere fluid, where, in the spirit of a Barker–Henderson prescription,[43] the hard-sphere segment-diameter has an efficient (temperature-dependent) diameter representing the soft repulsion of the interaction potential. In the PC-SAFT equation of state the pure component parameters of n-alkanes were determined based on a Lennard-Jones attractive potential, and universal model constants of the dispersion term were subsequently adjusted to the alkane series as archetype nonspherical nonpolar fluids. The soft repulsion was represented by an expression proposed by Chen and Kreglewski. This choice is pragmatic, because this expression compensates to some extent the omitted temperature dependence of correlation integrals of the dispersion term. The pure component parameters characterizing a nonpolar fluid in the PC-SAFT equation of state are the segment number m, the Lennard-Jones segment-size parameter σ, and the segment-dispersive energy parameter ϵ/k.

The dipolar and quadrupolar interactions are considered assuming point-multipole moments. The equation-of-state expressions are based on a third-order perturbation theory that was parametrized to comprehensive molecular simulation data for two-center Lennard-Jones fluids.[44–46] For mo-

lecular elongations up to two segments, the molecular model is well defined and the multipole moments (dipole and quadrupole moment) are assumed to be aligned along the molecular axis.[44] For molecules with more than two segments the multipolar interactions are assumed to only stretch between two segments. The molecular model then gets coarse grained because the positioning and orientation of the multipole moments are not further detailed. The two parameters, the dipole moment μ^D and the quadrupole moment Q, can suitably be approximated from quantum chemical calculations or from experiments.[44–46] Although the vacuum values do not do justice to the higher effective dipole moment in a dense fluid phase, the vacuum values can (at least for purposes of correlations) be used. This can be attributed to the observation that induced dipolar interactions can for pure fluids be well "hidden" as quasidispersive attractions.[47]

III. CLASSICAL DENSITY FUNCTIONAL THEORY

Interfaces can conveniently be studied in terms of the variables $\{V, T, \mu\}$, i.e., volume, temperature, and the chemical potential. The appropriate thermodynamic potential is the grand potential $\Omega(V, T, \mu)$, which, in the absence of an external field, is

$$\Omega = F[\rho(\tilde{\mathbf{r}})] - \mu \int d\tilde{\mathbf{r}} \rho(\tilde{\mathbf{r}}), \tag{3}$$

where $F[\rho(\tilde{\mathbf{r}})]$ is the Helmholtz energy and is a functional of the molecular density $\rho(\tilde{\mathbf{r}})$. Here, $\tilde{\mathbf{r}}$ is the vector giving the position as well as the configuration of a molecule and $\rho(\tilde{\mathbf{r}})$ is the density of molecules characterized by $\tilde{\mathbf{r}}$. We will later be concerned with the segment-chain structure of fluids, where $\mathbf{r}$ without the tilde $(\tilde{\ })$ will denote only the positional vector. Among all possible density profiles $\rho(\tilde{\mathbf{r}})$ the equilibrium density profile $\rho_{eq}(\tilde{\mathbf{r}})$ is the one that minimizes the grand potential, with

$$\left(\frac{\delta\Omega}{\delta\rho(\tilde{\mathbf{r}})} \right)_{\rho(\tilde{\mathbf{r}})=\rho_{eq}(\tilde{\mathbf{r}})} = 0. \tag{4}$$

The equilibrium density profile is then obtained by

$$0 = \frac{\delta F[\rho]}{\delta\rho(\tilde{\mathbf{r}})} - \mu. \tag{5}$$

For a compact notation we omit the index "eq" for the equilibrium density profile. The Helmholtz energy functional is decomposed into an ideal gas contribution and the residual part, with

$$F[\rho] = F^{ig}[\rho] + F^{res}[\rho]. \tag{6}$$

The ideal gas contribution is known exactly in the semi-classical limit, with

$$F^{ig}[\rho]/kT = \int d\tilde{\mathbf{r}} \rho(\tilde{\mathbf{r}})\{\ln[\rho(\tilde{\mathbf{r}})\Lambda^3] - 1\}, \tag{7}$$

and with

$$\frac{\delta F^{ig}[\rho]/kT}{\delta\rho(\tilde{\mathbf{r}})} = \ln[\rho(\tilde{\mathbf{r}})\Lambda^3], \tag{8}$$

where Λ is the de Broglie wavelength that here contains the translational and internal degrees of freedom. Because the ideal-gas term of chain fluids will be discussed below, we emphasize that an application of Eq. (7) would require a nontrivial integration over the configurational space of the chain molecules. The TPT1, however, allows for a simple procedure for the ideal gas term, as shown below.

The DFT is here applied to chain fluids composed of spherical segments. The configuration of these fluids is in an averaged way captured only by the position vector $\mathbf{r}$ of the segments.[48] The following equations are therefore formulated in terms of the segment density ρ_s and the molecular density ρ, with $\rho_s(\mathbf{r})=m\rho(\mathbf{r})$. This definition is for homonuclear fluids (i.e., fluids comprising segments of the same type) where the averaging does not for example distinguish between a terminal segment or a segment with two neighbor segments. Equation (5) can now be rewritten in terms of residual quantities, as

$$0 = \frac{\delta F^{res}[\rho]/kT}{\delta\rho(\mathbf{r})} + \ln[\rho(\mathbf{r})] - \mu_{b,L}^{res}/kT - \ln[\rho_{b,L}], \tag{9}$$

where $\rho_{b,L}$ is the bulk molecular density of the liquid phase, and $\mu_{b,L}^{res}$ is the corresponding residual chemical potential. The equilibrium density profile is obtained from Eq. (9) by iteration. In the simplest case this can be a Picard-iteration scheme (direct substitution), which is obtained by rearranging Eq. (9) as

$$\rho(\mathbf{r}) = \rho_{b,L}\exp\left(\mu_{b,L}^{res}/kT - \frac{\delta F^{res}[\rho]/kT}{\delta\rho(\mathbf{r})}\right). \tag{10}$$

In a straightforward DFT approach one strives for a suitable Helmholtz energy functional $F[\rho]$ for the problem at hand and perturbation schemes are often applied. In our case, we target at using the PCP-SAFT equation of state for calculating bulk properties, supplementing it with a suitable DFT formalism.

The PCP-SAFT equation of state is used for calculating the residual chemical potential in Eq. (10). It is given as the sum of several contributions as

$$\mu^{res} = \mu^{hs} + \mu^{chain} + \mu^{disp} + \mu^{multipolar}. \tag{11}$$

The Carnahan–Starling equation is applied for the hard-sphere contribution to the chemical potential μ^{hs}. The chain term accounts for the bonding of spherical segments to form chain fluids. The chain contribution, μ^{chain}, is based on Wertheim's TPT1.[7] The contribution for the dispersive attraction, μ^{disp}, was developed for chain molecules.[17] The multipolar contribution to the chemical potential, $\mu^{multipole}$, accounts for the electrostatic interactions due to dipolar and quadrupolar interactions of spherical and elongated fluids. For details on the PCP-SAFT equation of state and the equations for the chemical potential, we refer to Refs. 17, 44–46, and 49.

The PCP-SAFT equation of state was developed to correlate bulk properties and it is an equation of state, $F(\rho_b, T)$, formulated in terms of bulk densities ρ_b. An appropriate DFT

treatment requires a formulation of the Helmholtz energy for inhomogeneous fluids, leading to a functional $F[\rho(\mathbf{r}); T]$, as

$$\frac{\delta F^{res}[\rho]/kT}{\delta\rho(\mathbf{r})} = \frac{\delta F^{hs}[\rho]/kT}{\delta\rho(\mathbf{r})} + \frac{\delta F^{chain}[\rho]/kT}{\delta\rho(\mathbf{r})} + \frac{\delta F^{disp}[\rho]/kT}{\delta\rho(\mathbf{r})}$$
$$+ \frac{\delta F^{multipolar}[\rho]/kT}{\delta\rho(\mathbf{r})}. \tag{12}$$

For the multipolar contribution in Eq. (12) the local density approximation (LDA) is applied, so that $F^{multipolar}[\rho] = \int f^{multipolar}(\rho, T)d\mathbf{r}$. Here, $f^{multipolar}$ is the Helmholtz energy density, which is a function of the local density, not a functional. The functional derivative then simply gives $\delta F^{multipolar}[\rho]/\delta\rho(\mathbf{r}) = \mu^{multipolar}(\rho)$. Associating substances are not investigated here so that the association term is zero. We will now consider the remaining contributions to the Helmholtz energy functional $F[\rho(\mathbf{r}); T]$ corresponding to the PCP-SAFT equation of state

A. The hard-sphere contribution

The modified FMT provides an accurate description of inhomogeneous hard-sphere fluids.[35–37] For homogeneous fluids it simplifies to the Carnahan–Starling equation and it is thus compatible with the PCP-SAFT equation of state. According to the FMT the residual Helmholtz energy functional $F^{hs}[\rho(\mathbf{r})]$ of a hard-sphere fluid has the form

$$\frac{F^{hs}[\rho]}{kT} = \int \frac{f^{hs}(\mathbf{r})}{kT}d\mathbf{r}, \tag{13}$$

where the residual Helmholtz energy density f^{hs} is a function of local weighted densities only. For the detailed expressions of the FMT we refer to the original literature. The integrals appearing in the FMT can for a flat interface best be reduced to one-dimensional expressions by adopting cylindrical coordinates. For a fluid with a temperature-dependent effective hard-sphere diameter, $d(T) = \sigma(1 - 0.12\exp(-3(\epsilon/kT)))$, these expressions are summarized in Appendix A.

B. The chain contribution

Chapman and co-workers[26,27,39] proposed a functional based on Wertheim's TPT1 to account for the connectivity of spherical segments to form necklacelike chains. Before turning to the residual Helmholtz energy contribution due to chain connectivity, we have to be concerned with the ideal-gas reference state. The conformal degrees of freedom would normally lead to a contribution to the ideal-gas term in Eq. (7). Instead we follow the suggestion of Tripathi and Chapman[26] to treat the chain structure of the fluid in the ideal gas limit using the TPT1 of Wertheim. This is an elegant approach, because the conformational structure of a chain fluid is otherwise tedious to obtain. We have to revisit the ideal gas contribution, but now of the individual (non-bonded) segments of the chain. For this case, we introduce the superscript "IG" for the ideal gas contribution, with

$$F^{IG}[\rho]/kT = \int d\mathbf{r}\,m\rho(\mathbf{r})\{\ln[\rho(\mathbf{r})\Lambda^3] - 1\} \tag{14}$$

and

$$\frac{\delta F^{\mathrm{IG}}[\rho]/kT}{\delta\rho(\mathbf{r})} = m\,\ln[\rho(\mathbf{r})\Lambda^3], \tag{15}$$

where m is the number of segments comprising a chain. This ideal-gas contribution of the nonbonded segments is appropriate together with a TPT1 chain term because it also captures the ideal-gas contribution of chain formation. This chain term is indicated by the capital-letter superscript "CHAIN." Then, $F^{\mathrm{ig}} + F^{\mathrm{chain}} = F^{\mathrm{IG}} + F^{\mathrm{CHAIN}}$ and the regular chain term, analogous to the one used in the PCP-SAFT equation of state, is

$$\frac{\delta F^{\mathrm{chain}}[\rho]/kT}{\delta\rho(\mathbf{r})} = (m-1)\ln[\rho(\mathbf{r})] + \frac{\delta F^{\mathrm{CHAIN}}[\rho]/kT}{\delta\rho(\mathbf{r})}. \tag{16}$$

This equation with Eq. (12) can be used in Eq. (10). The last term was given[26] as

$$F^{\mathrm{CHAIN}}[\rho(\mathbf{r})]/kT = -(m-1)\int d\mathbf{r}\rho(\mathbf{r})$$
$$\times\{\ln[y^{dd}(\bar{\rho}(\mathbf{r}))\lambda(\mathbf{r})] - 1\}, \tag{17}$$

where $y^{dd}(\bar{\rho}(\mathbf{r}))$ is the cavity correlation function evaluated at contact distance d between segments. The cavity correlation function $y^{dd}(\bar{\rho}(\mathbf{r}))$ across interfaces is not well known; the behavior of a bulk phase at a mean local density is assumed. The cavity correlation function at contact distance is equal to the radial distribution function of unbonded spheres at contact distance and we apply the expression of Carnahan and Starling.[50] The average density appearing in the cavity correlation function at contact is simply the space-fixed average density in the interpenetration volume of two segments around position $\mathbf{r}$ with

$$\bar{\rho}(\mathbf{r}) = \frac{3}{4\pi d^3}\int_{|\mathbf{r}-\mathbf{r}'|<d} d\mathbf{r}'\rho(\mathbf{r}')$$
$$= \frac{3}{4\pi d^3}\int d\mathbf{r}'\rho(\mathbf{r}')\Theta(d-|\mathbf{r}-\mathbf{r}'|), \tag{18}$$

where in the second equality, we introduced a Heaviside function Θ. The cavity correlation function according to Carnahan–Starling is for an average density $\bar{\rho}(\mathbf{r})$ calculated as

$$y^{dd}(\bar{\rho}(\mathbf{r})) = \frac{1 - 0.5\bar{\eta}(\mathbf{r})}{(1 - \bar{\eta}(\mathbf{r}))^3}, \tag{19}$$

with a locally averaged dimensionless segment density (also termed "packing fraction")

$$\bar{\eta}(\mathbf{r}) = \frac{\pi}{6}\bar{\rho}(\mathbf{r})md^3. \tag{20}$$

The abbreviation $\lambda(\mathbf{r})$ appearing in Eq. (17) is the average density at contact distance around a segment with position $\mathbf{r}$, given as

$$\lambda(\mathbf{r}) = \frac{1}{4\pi d^2}\int d\mathbf{r}'\rho(\mathbf{r}')\delta(d-|\mathbf{r}-\mathbf{r}'|), \tag{21}$$

with δ as the Dirac function.

The derivative of the Helmholtz energy Eq. (17) is obtained with Eqs. (18) and (21) applying the product and chain rule of functional differentiation. The pair correlation function $y^{dd}(\bar{\rho}(\mathbf{r}))$ is a function (not a functional) of the mean density. With this, the derivative of Eq. (17) gets

$$\frac{\delta F^{\mathrm{CHAIN}}[\rho]/kT}{\delta\rho(\mathbf{r})}$$
$$= -(m-1)\{\ln[y^{dd}(\bar{\rho}(\mathbf{r}))\lambda(\mathbf{r})] - 1\}$$
$$- (m-1)\int d\mathbf{r}'\rho(\mathbf{r}')\frac{\partial\ln y^{dd}(\bar{\rho}(\mathbf{r}'))}{\partial\bar{\rho}(\mathbf{r}')}$$
$$\times\frac{3}{4\pi d^3}\Theta(d-|\mathbf{r}'-\mathbf{r}|)$$
$$- (m-1)\int d\mathbf{r}'\rho(\mathbf{r}')\frac{1}{\lambda(\mathbf{r}')}\frac{1}{4\pi d^2}\delta(d-|\mathbf{r}'-\mathbf{r}|). \tag{22}$$

C. The dispersive attraction

The starting point for the Helmholtz energy contribution due to dispersive attraction can for pairwise additive potentials be formulated exactly as

$$F^{\mathrm{PT}}[\rho(\mathbf{r});T]/kT$$
$$= \frac{1}{2}\int_0^1 d\varphi\sum_\alpha\sum_\beta\int\int d\mathbf{r}d\mathbf{r}'g_{\varphi,\alpha\beta}(\mathbf{r},\mathbf{r}';T)$$
$$\times\rho_\alpha(\mathbf{r})\rho_\beta(\mathbf{r}')\frac{u_{\alpha\beta}^{\mathrm{PT}}(\mathbf{r},\mathbf{r}')}{kT}, \tag{23}$$

where the indices α and β run over all segments of polysegmented molecule 1 and 2, respectively. The parameter φ is introduced to accomplish a continuous transition from the reference fluid to the target fluid, with $u(r) = u_0(r) + \varphi u^{\mathrm{PT}}(r)$. The direct applicability and practical use of Eq. (23) is limited by the fact that one would have to provide the pair correlation function $g_{\varphi,\alpha\beta}(\mathbf{r},\mathbf{r}';T)$ for the full bandwidth of fluids between the reference fluid and the target fluid. For cases where the pair correlation function of the reference fluid is similar to that of the target fluid, one can expand around the pair correlation function. For the dispersive attraction of simple fluids in bulk phases this condition is reasonably well justified when reference fluids with hard repulsion are considered; the perturbation expansion then converges quickly. We assume hard chains as the reference fluid. We simplify the treatment by not resolving the difference in the local density of various segments in the chain,[48] so that $\rho_\alpha(\mathbf{r}) = \rho(\mathbf{r})$. The distinction between a terminal segment of a chain and a segment located in the middle of a chain is not preserved with this approximation. For inhomogeneous conditions, the (hard-chain) pair correlation function is not well known and we approximate it in several ways. (1) Following Ref. 51 we assume the segment pair correlation function of the homogeneous fluid at the average of the densities in $\mathbf{r}$ and $\mathbf{r}'$, with $\hat{\rho} = (1/2)(\rho(\mathbf{r}) + \rho(\mathbf{r}'))$. And (2) we consider an average over the segment pair correlation func-

tion. The average segment-segment radial distribution is

$$g^{hc}(\hat{r},\hat{\rho}) = \frac{1}{m^2}\sum_{\alpha}\sum_{\beta}g^{hc}_{\alpha\beta}(\hat{r},\hat{\rho}), \tag{24}$$

where the index (hc) refers to segments of the hard-chain fluid and $\hat{r}=|\mathbf{r}-\mathbf{r}'|$ is a segment-segment distance for segments on two different chain molecules. The first order perturbation term (index "1PT") then gets

$$F^{1PT}[\rho]/kT = \frac{1}{2}\int\int d\mathbf{r}d\mathbf{r}'m^2\rho(\mathbf{r})\rho(\mathbf{r}')g^{hc}(\hat{r},\hat{\rho})\frac{u^{PT}(\hat{r})}{kT}. \tag{25}$$

The functional derivative to the density is

$$\frac{\delta F^{1PT}[\rho]/kT}{\delta\rho(\mathbf{r})} = \int d\mathbf{r}'m^2\rho(\mathbf{r}')$$
$$\times\left[g^{hc}(\hat{r},\hat{\rho})+\frac{1}{2}\rho(\mathbf{r})\frac{\partial g^{hc}(\hat{r},\hat{\rho})}{\partial\hat{\rho}}\right]\frac{u^{PT}(\hat{r})}{kT}. \tag{26}$$

While this may be an appropriate approximation for the dispersion of chain fluids, it is not yet consistent with the PC-SAFT equation of state. The difference between Eq. (25) and the dispersion term of the PC-SAFT equation of state, however, is fairly small and we treat the difference locally.[40] A dispersion term that is compatible with the PC-SAFT equation of state is then

$$\frac{\delta F^{disp}[\rho]/kT}{\delta\rho(\mathbf{r})} = \frac{\delta F^{1PT}[\rho]/kT}{\delta\rho(\mathbf{r})} + \left(\frac{\mu^{disp,PC\text{-}SAFT}}{kT}-\frac{\mu^{1PT}}{kT}\right). \tag{27}$$

For the segment-segment radial distribution function of the hard-sphere fluid, $g^{hc}(m;r,\rho)$, we apply the Percus–Yevick approximation.[52,53] The integration in Eq. (26) is carried out numerically up to a cutoff radius $r_c=9\sigma$. In some calculations a second order perturbation term according to the prescription of Barker and Henderson applied to chain fluids is taken into account (Appendix B).

IV. SURFACE TENSION

The surface tension of the system is the difference of the grand potential of the interface and of the bulk phases, according to

$$\gamma = \frac{1}{A}(\Omega - \Omega_{bulk}), \tag{28}$$

where A denotes the surface area. The surface tension of a flat interface can conveniently be calculated from

$$\gamma_{DFT} = \int\{p_{bulk}+f[\rho(z)]-\mu\rho(z)\}dz, \tag{29}$$

where $f[\rho(z)]$ is the Helmholtz energy density in unit [J m^{-3}], defined as $F[\rho(z)]=\int f[\rho(z)]Adz$. The subscript has been introduced to the surface tension in Eq. (29) in order to indicate that this is the surface tension of a planar interface in the absence of long-range capillary waves.

V. CAPILLARY WAVE CONTRIBUTION

The DFT formalism has been applied with the assumption of a flat interface. The spontaneous occurrence of capillary waves of free vapor-liquid interfaces is thereby omitted. The capillary waves are due to thermal fluctuations and exist over a wide range of length scales, from microscopic to macroscopic length. Capillary waves have to lower the grand potential Ω because they form spontaneously and according to Eq. (28) they lower the surface tension of any free surface, compared to a flat interface. Meunier developed a mode-coupling theory,[54] where the average amplitude of the mode with wave vector $|\mathbf{q}|=q$ is

$$\langle\zeta_q^2\rangle = kT(\Delta\rho_m g + \gamma(q)q^2 + K(q)q^4)^{-1}, \tag{30}$$

where $\Delta\rho_m$ is the mass-density difference, g is the gravitational acceleration, and $K(q)$ denotes the rigidity constant for the curvature of the interface due to the capillary waves. According to the mode coupling theory,[54] both the surface tension $\gamma(q)$ and the rigidity $K(q)$ are functions of the wavelength, with the surface tension

$$d\gamma(q) = \frac{3}{4\pi}kTqdq. \tag{31}$$

This equation can be integrated between two values of the wave vector. A value of the wave vector of $q=0$ corresponds to waves of infinite length and the corresponding surface tension $\gamma=\gamma(q=0)$ is the macroscopic surface tension that is measured experimentally. The macroscopic surface tension is the target of our calculations. Integration of Eq. (31) (from 0 to q^{max}) gives

$$\gamma = \gamma(q^{max}) - \frac{3}{8\pi}kT(q^{max})^2. \tag{32}$$

The DFT calculations lead to a density profile where some of the fluctuations are already accounted for. This requires the definition of a cutoff value for the wave-vector q^{max}. Wavelength contributions up to $1/q^{max}$ are captured by the interfacial density profile of the DFT formalism [with $\gamma(q^{max})=\gamma_{DFT}$]; wavelengths greater $1/q^{max}$ need to be added in order to estimate experimental surface tensions. A unified molecular theory bridging a van der Waals approach (or more general a DFT approach) to capillary wave theory is yet to be developed[55–57] and some ambiguity is inherent in the choice of the cutoff value q^{max}. Meunier, however, made progress by applying several assumptions. At the critical point, interfaces get nonridged ($K(q)=0$) and Eq. (30) simplifies. Further, an approximation of the cutoff value q^{max} based on the surface tension can be devised when considering the scaling laws around the critical point. The temperature dependence of the surface tension γ and the correlation length ξ in the vicinity of the critical point is

$$\gamma = \gamma_0 \left(\frac{T_c - T}{T_c} \right)^{2\nu} + \cdots, \tag{33}$$

$$\xi = \xi_0 \left(\frac{T_c - T}{T_c} \right)^{-\nu} + \cdots, \tag{34}$$

with $\nu = 0.63$. Only the first order terms of the expansions are here considered. Moldover[58] analyzed the amplitude ratio

$$\frac{\gamma_0 \xi_0^2}{kT_c} = \kappa \tag{35}$$

for several components based on experimental data and gave an average value of $\kappa = 0.386$. With this value and assuming the Fisk–Widom theory[59] for the diffuse interface (equivalent to the interfacial profile here calculated from DFT), the cutoff is then $q^{max} = 1/(2.55\xi)$. Values for ξ_0 are available for some components[58] and one could, with Eq. (34), evaluate the capillary-wave contribution to the surface tension. This approach has been taken by Kahl and Winkelmann,[60] but their empirical exponent $2\nu < 1$ in the reduced temperature of the capillary wave contribution leads to negative surface tensions when approaching the critical point. Moreover, the ξ_0 values vary significantly for various components and a different approach is here taken. From Eq. (35) with Eqs. (33) and (34) one gets $\xi^2 = \kappa kT_c / \gamma$ to first order around the critical point. Inserting this into Eq. (32) finally gives a simple approximation for the macroscopic surface tension

$$\gamma = \gamma_{DFT} \left(1 + \frac{3}{8\pi} \frac{T}{T_c} \frac{1}{(2.55)^2} \frac{1}{\kappa} \right)^{-1}. \tag{36}$$

The experimental data for the amplitude ratio κ are more well behaved than the values ξ_0 so that this formulation should be suited for a variety of substances.[58] The values of κ still show quite some scattering and the less ambiguous value $\kappa = 0.24$ from the Ising model[61,58] is here adopted. Equation (36) has been derived for conditions valid in the immediate vicinity of the critical point. However, if the first-order scaling law Eq. (33) is applied far from the critical point with constant γ_0 (even down to the triple point temperature) one empirically finds good agreement to experimental data. This encourages, if one is determined enough, the use of Eq. (36) at conditions away from the critical point and we assume Eq. (36) valid over the whole vapor-liquid region.

VI. NUMERICAL PROCEDURE

The DFT calculations described here require the iteration of a density profile of chain segments across a planar vapor-liquid interface. The interface is spatially discretized in, typically, 1000 grid points covering a width of 50σ, leading to a grid spacing of 0.02σ. The cutoff distance for the numerical integration was set to $r_c = 9\sigma$ and the grid was extended by the same distance to the left and to the right sides, without, however, altering the density values at these extended regions. The radial distribution function of hard chains,

$g^{hc}(r, \rho)$, was assumed to be unity at distances $r > 4\sigma$, so that a substantial part of the integration of the dispersion term can be performed analytically. The density profile was iterated by an inversion procedure that is not further detailed here. However, a simple damped direct substitution algorithm (Picard iteration) was also implemented and was found to give identical results.

For the starting density profile a simple empirical relation was parametrized, which gives excellent starting values for all investigated cases (be it spherical fluids or chain fluids), with

$$\rho^{(0)}(z) = \frac{1}{2}(\rho_{bulk,L} - \rho_{bulk,V}) \tanh \left(2.7 \frac{z}{\sigma} \left(\frac{T_c^{calc} - T}{T_c^{calc}} \right) \right)$$
$$+ \frac{1}{2}(\rho_{bulk,L} + \rho_{bulk,V}). \tag{37}$$

The calculation followed six steps for a given temperature.

(1) Determine the critical temperature T_c^{calc} of the considered fluid.
(2) Determine the bulk residual chemical potential and the bulk densities of both coexisting phases.
(3) Generate the starting density profile according to Eq. (37).
(4) For the given segment number m, generate values for the pair correlation function $g^{hc}(\hat{r}, \hat{\rho})$ and the derivative to density $(\partial g^{hc}(\hat{r}, \hat{\rho}) / \partial \hat{\rho})$ in a two-dimensional grid of $\{\hat{r}, \hat{\rho}\}$ and parametrize a cubic spline interpolation.
(5) Iterate $\rho(z)$ to desired accuracy, by solving Eq. (10).
(6) Calculate the surface tension from Eqs. (29) and (36).

VII. RESULTS AND DISCUSSION

This chapter analyzes several aspects of the above DFT approach. First, the capillary wave contribution to the surface tension is evaluated. Second, the mean-field approximation of the dispersion term is compared to a non-mean-field approach of first order. Third, the contribution of the second order perturbation term is evaluated. Some n-alkanes are thereby considered as prototypical for nonspherical, nonpolar, and nonassociating substances. Subsequently, the capillary-wave contribution is reparametrized and the resulting model is applied to some further real systems. Nonpolar and polar fluids are considered. Associating fluids usually have both a (local) dipole moment and H-bonding sites. In order to single out the effect of dipolar interactions, we limit the consideration to nonassociating substances. The pure component parameters for all calculations are taken from Refs. 17, 44, and 45.

Figure 1 shows results of the DFT with and without the capillary wave contribution in comparison with experimental data of three n-alkanes. The capillary wave contribution lowers the surface tension and leads to an improved representation of the experimental data, particularly for smaller chain length.
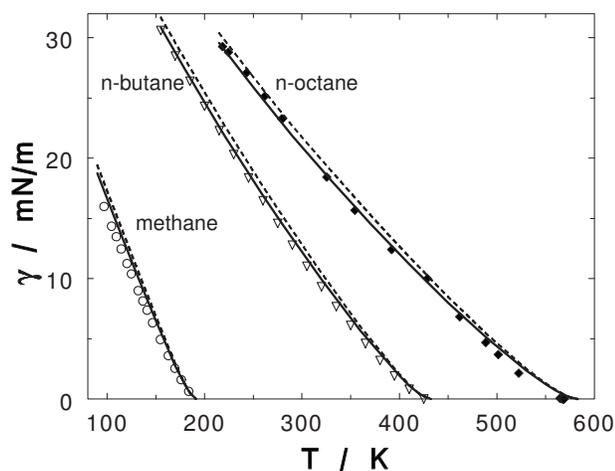
FIG. 1. Comparison of the DFT with capillary wave contribution according to the parameters of Meunier (Ref. 54) (solid line) and of the "intrinsic" surface tension from DFT (dashed line) to experimental data for surface tension of three alkanes (symbols).

FIG. 3. Comparison of the first-order perturbation theory (solid line) to the second-order perturbation theory (dashed line). The calculations are for methane as a representative example illustrating the small second-order contribution.

The effect of the non-mean-field perturbation term is examined in Fig. 2. The first-order non-mean-field perturbation theory [Eqs. (26) and (27)] is for three n-alkanes compared to the mean-field approach (where $g^{hc}=1$ is assumed). The surface tension calculated from the mean-field assumption does not show the right temperature behavior. The full perturbation term, on the other hand, improves on this deficiency and leads to results in good agreement with experimental data, so that the curve for the surface tension is steeper at low temperatures, in good agreement with experimental data.

Since the non-mean-field approach improves the results compared to the mean-field formulation, it is interesting to investigate the effect of a further model refinement, where the second-order perturbation term of the dispersive interactions is taken into account. The second order term is described in Appendix B and a comparison of the first-order theory versus the second-order approach is given in Fig. 3. The second-order contribution is seen to lead to a marginally

different result and we conclude that a second-order correction is not needed. The calculations in Fig. 3 are for methane but the result is representative also for higher alkanes. The small contribution of the second order term is in contrast with a regular perturbation theory [without the correction of the second term in Eq. (27)], where the second order term is known to significantly contribute[62] to the surface tension. The perturbation theory according to Eq. (27) is thus very forgiving with respect to the (nonlocal) perturbation theory. That is due the second term of Eq. (27), where any deviation of a nonlocal perturbation theory to the PC-SAFT equation of state is corrected. The LDA that is considered in this correction is seen to be sufficiently accurate. It is worth mentioning that the approach [Eq. (27)] is also fairly insensitive to the effective hard-sphere diameter: if a hard-sphere diameter is defined by integrating the repulsive part of the Lennard-Jones potential according to the Barker–Henderson prescription, instead of using the Chen–Kreglewski expression, we find again very similar results (not shown).

The derivation of Eq. (36) is based on the Fisk–Widom theory, so that the capillary-wave contribution is only approximately compatible with our approach. Moreover, the values for the amplitude ratio κ show quite some scattering.[58] Values for κ are therefore adjusted to experimental data of surface tensions, with the *ad hoc* assumption that κ depends only linearly on the chain length. From the n-alkane series we find $\kappa(m)=0.0045+0.0674m$. Individually optimized values of κ are well correlated with the linear dependence on segment number m and the values are in a range similar to the ones reported from experiments and the Ising model for the critical region. Nonetheless, we note that κ degenerates to a model parameter and loses some of its meaning as the amplitude ratio. The increase in the κ-parameter with chain length leads to a vanishing contribution of capillary waves for polymeric fluids. We applied this approach to argon and xenon in order to confirm that κ does not dependent on the segment size parameter σ. Quantitative agreement was thereby found (not shown) for the surface
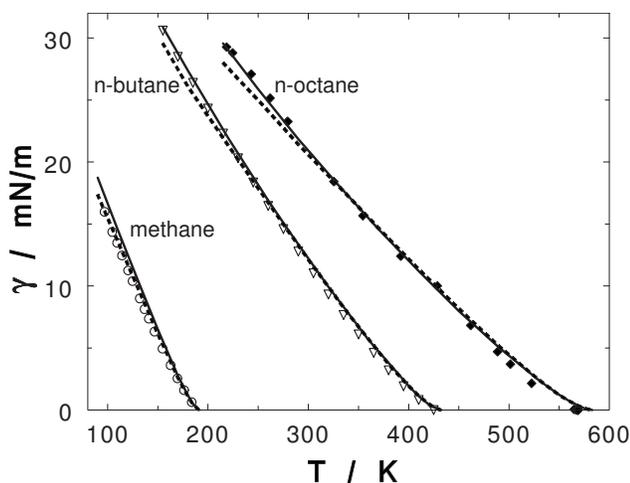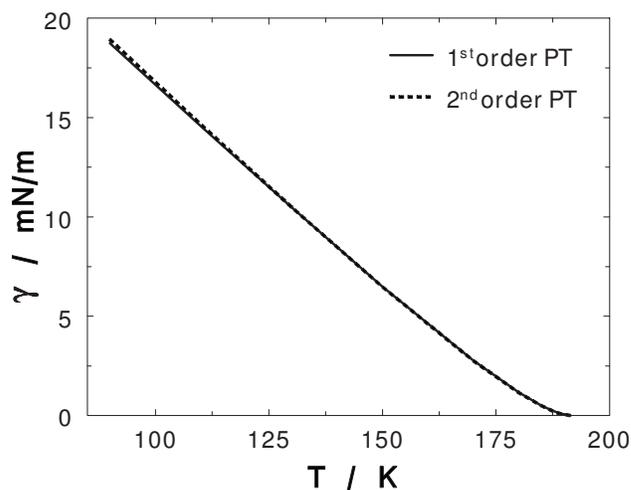

FIG. 2. Comparison of the non-mean-field DFT (solid line) and the mean-field DFT (dashed line) to experimental data for surface tension of three alkanes (symbols).
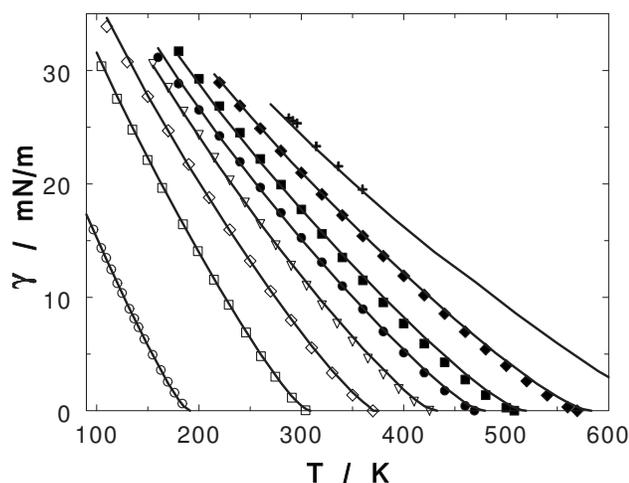
FIG. 4. Surface tension of n-alkanes: comparison of the PC-SAFT-DFT model (solid line) to experimental data (symbols) of methane, ethane, propane, n-butane, n-pentane, n-hexane, n-octane, and n-dodecane (from left to right).
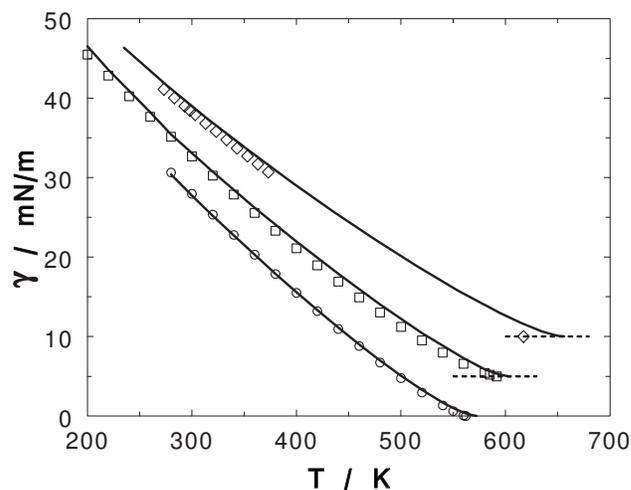

FIG. 5. Surface tension of aromatic compounds: comparison of the PC-SAFT-DFT model (solid line) to experimental data of benzene (Ref. 64) (spheres), toluene (Ref. 65) (squares), and propyl-benzene (Ref. 66) (diamonds). For clarity two of the data sets are shifted up by 5 and 10 mN/m, respectively.

tension of these fluids without an adjustable parameter. For further tests of the model, the shorthand notation "PC-SAFT-DFT" will be used for the non-mean-field first-order perturbation DFT with the PC-SAFT equation of state together with this capillary-wave contribution. A similarly cryptic acronym, namely, PCP-SAFT-DFT refers to the same model, where however the polar terms of the PCP-SAFT model are taken into account.

A comparison of the PC-SAFT-DFT approach to experimental surface tensions of some n-alkanes[63] is shown in Fig. 4 and very good agreement is thereby found. The PC-SAFT equation of state performs relatively well in describing the critical point of fluids, even without a renormalization. An adequate description of the critical temperature is a prerequisite for an appropriate representation of the surface tension, which underpins the advantage of applying a dispersion term in the form of Eq. (27) where a suitable bulk-phase equation of state can be combined with a relatively simple perturbation term.

The results of the mean-field approximation are not shown in Fig. 4; but the results, even with individually adjusted κ values, are significantly weaker compared to the non-mean-field version. An inaccurate shape of the surface-tension curve was already observed in Fig. 2.

The PC-SAFT-DFT model is then applied to some other classes of substances in order to investigate the predictive capabilities of the model. Surface tensions of benzene, toluene, and propyl-benzene as three representative aromatic compounds are shown in Fig. 5. No parameter is adjusted to interfacial properties for these systems and the agreement with the experimental data is very good. Similar to the study of Fu and Wu,[24] a rescaling of parameters (as in Ref. 48) or readjusting pure-component parameters including surface tension data (as in Ref. 42) is not needed for this approach. Some deviations appear for n-propyl-benzene, where, however, the model also overestimates the critical point more than usual.

A comparison of the PC-SAFT-DFT model with three

ethers and three ethanoates is given in Figs. 6 and 7, respectively. Based again only on the pure component parameters determined from bulk properties, the model predicts surface tensions in close agreement with the experimental data.

Some deviation of the PC-SAFT-DFT model appears for dimethyl-ether in Fig. 6, which indicates that dipolar fluids require a model refinement. This is confirmed for acetone, as a strongly polar, nonassociating substance. The comparison of the PCP-SAFT-DFT model to experimental data of acetone in Fig. 8 reveals a higher deviation. Even higher deviations are seen for the model, when the dipolar interactions are not explicitly accounted for (PC-SAFT-DFT). Although the dipole term of the PCP-SAFT equation of state together with the LDA for the DFT treatment improve the description of the surface tension, one in fact has to expect some deviation for strongly polar substances. That is because the orien-
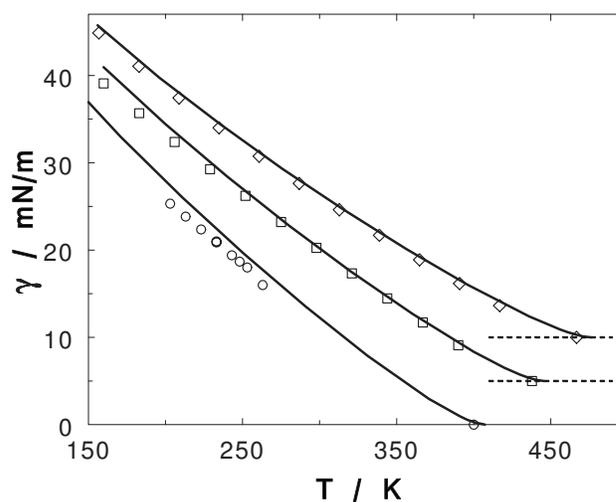

FIG. 6. Surface tension of ethers: comparison of the PC-SAFT-DFT model (solid line) to experimental data of dimethyl-ether (Ref. 67) (spheres), methyl-ethyl-ether (Ref. 68) (squares), and diethyl-ether (Ref. 68) (diamonds). For clarity two of the data sets are shifted up by 5 and 10 mN/m, respectively.
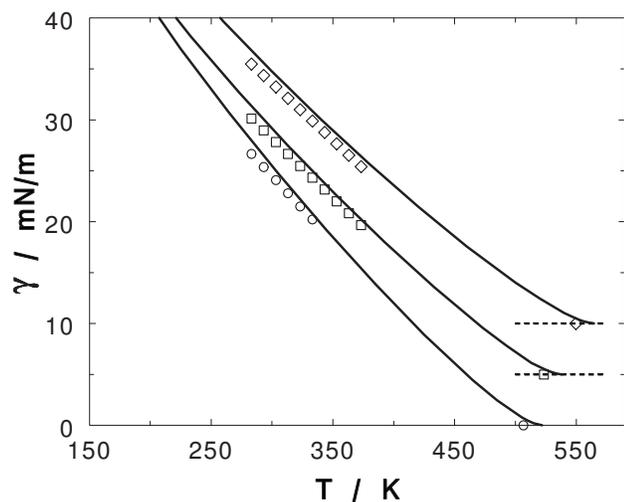
FIG. 7. Surface tension of ethanoates: comparison of the PC-SAFT-DFT model (solid lines) to experimental data (Ref. 67) for methyl-ethanoate (spheres), ethyl-ethanoate (squares), and propyl-ethanoate (diamonds). For clarity two of the data sets are shifted up by 5 and 10 mN/m, respectively.

FIG. 9. Surface tension of carbon dioxide: comparison of the PCP-SAFT-DFT model (solid lines) and of the nonpolar PC-SAFT-DFT (dashed line) to experimental data (Ref. 77) (symbols).

tational distribution of dipoles across the interface is not resolved in our approach. A fluid of dipoles actually lowers its grand potential $\Omega(V, T, \mu)$ by a nonisotropic orientational distribution in inhomogeneous systems.[69–75] This leads to a lower surface tension compared to a case where a uniform orientational distribution function is assumed. A further study will have to show whether a simple mean-field assumption to account for the orientational distribution of dipoles, as worked out by Refs. 69–71, is sufficient to get to a more quantitative agreement for dipolar components.

Carbon dioxide is a archetype strongly quadrupolar substance. Figure 9 compares calculated surface tension of carbon dioxide to experimental data, in order to evaluate whether model deficiencies, as identified for strongly dipolar substances, also get apparent for strongly quadrupolar fluids. The proposed functional, however, is in very good agreement with the experimental data which suggests that the charge distribution of quadrupoles is effectively screened across in-

terfaces. Results for the functional applying the nonpolar PC-SAFT equation of state are shown in the same diagram. The result of this model is weak in comparison with the PCP-SAFT-DFT variant, confirming that polar interactions should explicitly be taken into account in the equation of state.

VIII. CONCLUSION

A Helmholtz energy functional for inhomogeneous fluid phases based on a first-order perturbation theory for the dispersive interactions of nonspherical components is proposed. The difference of the perturbation theory to the dispersion term of the PCP-SAFT equation of state is treated with a LDA, as suggested by Gloor et al.[40] The resulting functional is compatible with the PCP-SAFT equation of state. A non-mean-field first-order perturbation theory was seen to improve the results compared to a mean-field approach, whereas a nonlocal second order perturbation term does not contribute significantly to the results. A simple model for the capillary wave contribution to the surface tension of a vapor-liquid interface is proposed. This model is based on a first order expansion of the universal critical scaling behavior.

The capillary wave contribution was reparametrized to experimental surface tensions of n-alkanes and the resulting model, when applied to nonpolar or only moderately polar fluids, gives excellent results for the surface tension. Rescaling of pure component parameters or readjusting pure component parameters together with surface tension data is not needed for the proposed model.

The polar interactions are treated with a LDA. Excellent results are obtained with this approach for carbon dioxide as a strongly quadrupolar fluid, whereas the nonpolar variant of the model (PC-SAFT-DFT) leads to a weaker results. The surface tension of acetone, as a prototypical dipolar fluid, however, is overpredicted by the model (although not as severe as the nonpolar variant of the model). This shows that the surface tension of acetone is lowered due to a nonisotropic molecular orientation. This effect remains to be taken
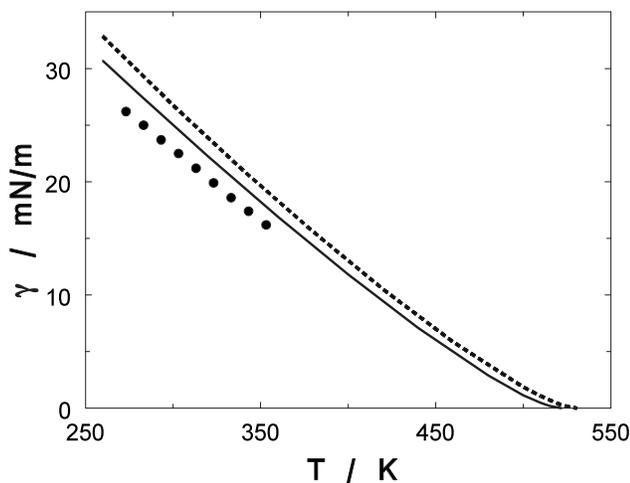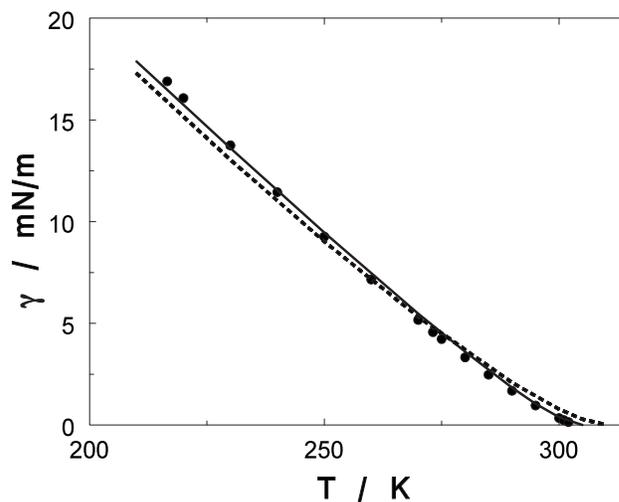

FIG. 8. Surface tension of acetone: comparison of the PCP-SAFT-DFT model (solid lines) and of the nonpolar PC-SAFT-DFT (dashed line) to experimental data (Ref. 76) (symbols).

into account by solving for the orientational distribution function leading to a minimal grand potential.

APPENDIX A: DFT FOR A PLANAR VAPOR-LIQUID INTERFACE

The general volume integrals of the hard-sphere and the chain terms can for the special case of planar interfaces be reformulated as one-dimensional integrals. The integrations are worked out in a cylindrical coordinate system with the z-coordinate normal to the interface.

1. Hard-sphere contribution

The functional derivative of the hard-sphere contribution Eq. (13) can for flat interfaces be written as

$$
\frac{\delta F^{\mathrm{hs}}[\rho]/kT}{\delta \rho(z)} = m \int_{-d/2}^{d/2} \left\{ \frac{1}{d} \frac{\partial \phi}{\partial n_0} + \frac{1}{2} \frac{\partial \phi}{\partial n_1} + \pi d \frac{\partial \phi}{\partial n_2} \right.
$$
$$
\left. + \pi \frac{\partial \phi}{\partial n_3} ((d/2)^2 - z'^2) \right\} dz'
$$
$$
+ m\mathbf{e}_z \int_{-d/2}^{d/2} \left\{ \frac{1}{d} \frac{\partial \phi}{\partial \mathbf{n}_{V1}} z' + 2\pi \frac{\partial \phi}{\partial \mathbf{n}_{V2}} z' \right\} dz', \tag{A1}
$$

where for convenience ϕ is defined as $\phi = f^{\mathrm{hs}}/kT$. The weighted densities n_α with $\alpha \in \{0 \cdots 3\}$ and the weighted vector densities $\mathbf{n}_\alpha$ with $\alpha \in \{V1, V2\}$ are for planar interfaces summarized below. The derivatives appearing in Eq. (A1) are evaluated at position $(z+z')$. These are

$$
\frac{\partial \phi}{\partial n_0} = -\ln(1-n_3), \tag{A2}
$$

$$
\frac{\partial \phi}{\partial n_1} = \frac{n_2}{1-n_3}, \tag{A3}
$$

$$
\frac{\partial \phi}{\partial n_2} = \frac{n_1}{1-n_3} + (3(n_2)^2 - 3(\mathbf{n}_{V2} \cdot \mathbf{n}_{V2}))
$$
$$
\times \frac{n_3 + (1-n_3)^2 \ln(1-n_3)}{36\pi(n_3)^2(1-n_3)^2}, \tag{A4}
$$

$$
\frac{\partial \phi}{\partial n_3} = \frac{n_0}{1-n_3} + \frac{n_1 n_2 - \mathbf{n}_{V1} \cdot \mathbf{n}_{V2}}{(1-n_3)^2} - ((n_2)^3 - 3n_2 \mathbf{n}_{V2} \cdot \mathbf{n}_{V2})
$$
$$
\times \frac{n_3((n_3)^2 - 5n_3 + 2) + 2(1-n_3)^3 \ln(1-n_3)}{36\pi(n_3)^3(1-n_3)^3}, \tag{A5}
$$

$$
\frac{\partial \phi}{\partial \mathbf{n}_{V1}} = -\frac{\mathbf{n}_{V2}}{1-n_3}, \tag{A6}
$$

$$
\frac{\partial \phi}{\partial \mathbf{n}_{V2}} = -\frac{\mathbf{n}_{V1}}{1-n_3} - 6n_2 \mathbf{n}_{V2} \frac{n_3 + (1-n_3)^2 \ln(1-n_3)}{36\pi(n_3)^2(1-n_3)^2}, \tag{A7}
$$

and the weighted densities are for pure hard-sphere fluids across a flat one-dimensional interface given as

$$
n_2(z) = \pi d \int_{-d/2}^{d/2} \rho_s(z+z') dz', \tag{A8}
$$

$$
n_0(z) = \frac{1}{\pi d^2} n_2(z), \tag{A9}
$$

$$
n_1(z) = \frac{1}{2\pi d} n_2(z), \tag{A10}
$$

$$
n_3(z) = \pi \int_{-d/2}^{d/2} \rho_s(z+z')((d/2)^2 - z'^2) dz', \tag{A11}
$$

$$
\mathbf{n}_{V2}(z) = 2\pi \mathbf{e}_z \int_{-d/2}^{d/2} \rho_s(z+z') z' dz', \tag{A12}
$$

$$
\mathbf{n}_{V1}(z) = \frac{1}{2\pi d} \mathbf{n}_{V2}(z), \tag{A13}
$$

where $\mathbf{e}_z$ denotes the unity vector in the z-direction.

2. The chain contribution

For a flat interface the integrals appearing in Eq. (22) can be reduced to one-dimensional form, as

$$
\frac{\delta F^{\mathrm{CHAIN}}[\rho]/kT}{\delta \rho(z)}
$$
$$
= -(m-1)\{\ln[y^{dd}(\bar{\rho}(z))\lambda(z)] - 1\}
$$
$$
- (m-1)\frac{3}{4d^3} \int_{-d}^{d} \rho(z_2) \frac{\partial \ln y^{dd}(\bar{\rho}(z_2))}{\partial \bar{\rho}(z_2)} (d^2 - z'^2) dz'
$$
$$
- (m-1)\frac{1}{2d} \int_{-d}^{d} \frac{\rho(z_2)}{\lambda(z_2)} dz', \tag{A14}
$$

where $z_2 = z + z'$. The average density appearing in the cavity correlation function is

$$
\bar{\rho}(z) = \frac{3}{4d^3} \int_{-d}^{d} \rho(z+z')(d^2 - z'^2) dz', \tag{A15}
$$

and the average density at contact distance is

$$
\lambda(z) = \frac{1}{2d} \int_{-d}^{d} [\rho(z+z') dz']. \tag{A16}
$$

3. The dispersive attraction

Starting from a space-fixed coordinate system, where the vector $\mathbf{r} = \{z, r, \theta\}$ is defined as illustrated in Fig. 10 we shift the coordinate system to $\{z, 0, 0\}$, because the flat interface is invariant to the radial and angular direction. The integration in the vector $\mathbf{r}'$ is carried out in an auxiliary coor-
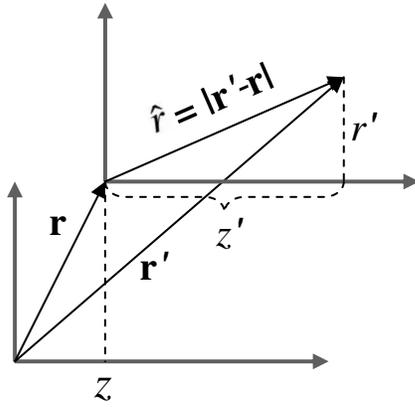
FIG. 10. Nomenclature of the coordinate systems for carrying out the integrations: the space-fixed coordinate system (below) and an auxiliary coordinate system (above).

dinate system at $\{z,0,0\}$ (see Fig. 10). The position $\mathbf{r}'$ is then $\mathbf{r}'=(z+z',r',\phi)$. We then substitute the radial integration (in r') for an integration in coordinate $\hat{r}=|\mathbf{r}'-\mathbf{r}|=\sqrt{z'^2+r'^2}$. Equation (26) then results in

$$\frac{\delta F^{1\text{PT}}[\rho]/kT}{\delta\rho(\mathbf{r})} = 2\pi \int_{-\infty}^{\infty} dz' m^2\rho(z+z') \int_{|z'|}^{\infty} d\hat{r}$$
$$\times \left[g^{\text{hc}}(\hat{r},\hat{\rho}) + \frac{1}{2}\rho(z)\frac{\partial g^{\text{hc}}(\hat{r},\hat{\rho})}{\partial\hat{\rho}} \right] \frac{u^{\text{PT}}(\hat{r})}{kT}\hat{r}. \tag{A17}$$

The integration in this equation is carried out numerically up to a cutoff radius r_c. At distances greater than r_c we assume the pair correlation function to be unity and the integration beyond r_c can be conducted analytically to give

$$\frac{\delta F^{1\text{PT}}[\rho]/kT}{\delta\rho(\mathbf{r})} = 2\pi \int_{-\infty}^{-r_c} dz' m^2\rho(z+z') \frac{\varepsilon}{kT}\left(\frac{2}{5}|z'|^{-10} - |z'|^{-4}\right)$$
$$+ 2\pi \int_{-r_c}^{r_c} dz' m^2\rho(z+z')\Psi(z,z')$$
$$+ 2\pi \int_{r_c}^{\infty} dz' m^2\rho(z+z')$$
$$\times \frac{\varepsilon}{kT}\left(\frac{2}{5}(z')^{-10} - (z')^{-4}\right), \tag{A18}$$

where an auxiliary function was defined, with

$$\Psi(z,z') = \int_{|z'|}^{r_c} d\hat{r}\left[g^{\text{hc}}(\hat{r},\hat{\rho}) + \frac{1}{2}\rho(z)\frac{\partial g^{\text{hc}}(\hat{r},\hat{\rho})}{\partial\hat{\rho}} \right] \frac{u^{\text{PT}}(\hat{r})}{kT}\hat{r}$$
$$+ \frac{\varepsilon}{kT}\left(\frac{2}{5}(r_c)^{-10} - (r_c)^{-4}\right). \tag{A19}$$

APPENDIX B: SECOND ORDER PERTURBATION THEORY

A second order perturbation theory of Barker and Henderson for the dispersive interactions of chain molecules is here formulated in functional form. The difference be-

tween this nonlocal theory and the PC-SAFT equation of state is again treated locally, so that a functional consistent with the PC-SAFT equation of state is

$$\frac{\delta F^{\text{disp}}[\rho]/kT}{\delta\rho(\mathbf{r})} = \frac{\delta F^{2\text{PT}}[\rho]/kT}{\delta\rho(\mathbf{r})} + \left(\frac{\mu^{\text{disp,PC-SAFT}}}{kT} - \frac{\mu^{2\text{PT}}}{kT}\right). \tag{B1}$$

The second order perturbation theory of Barker and Henderson in the macroscopic compressibility approximation for chain molecules is

$$F^{2\text{PT}}[\rho]/kT = \frac{1}{2}\int\int d\mathbf{r}d\mathbf{r}' m^2\rho(\mathbf{r})\rho(\mathbf{r}')g^{\text{hc}}(\hat{r},\hat{\rho})\frac{u^{\text{PT}}(\hat{r})}{kT}$$
$$- \frac{1}{4}\int d\mathbf{r}m^2\left(\frac{\partial\rho(\mathbf{r})}{\partial p^{\text{hc}}/kT}\right)\rho(\mathbf{r})^2$$
$$\times \int d\mathbf{r}' g^{\text{hc}}(\hat{r},\rho(\mathbf{r}))\left(\frac{u^{\text{PT}}(\hat{r})}{kT}\right)^2, \tag{B2}$$

where the compressibility in the second order term is approximated locally, because the second order term is relatively short ranged. In this study, it is concluded, however, that the second order term can be neglected without a significant error if a functional of the form of Eq. (27) or Eq. (B1) is used.

[1] J. S. Rowlinson and B. Widom, *Molecular Theory of Capillarity* (Oxford University Press, Oxford, 1989).
[2] R. Evans, *Fundamentals of Inhomogeneous Fluids* (Dekker, New York, 1992), Chap. 3.
[3] H. T. Davis, *Statistical Mechanics of Phases and Interfaces, and Thin Films* (VCH, Weinheim, 1996).
[4] J. Z. Wu, AIChE J. **52**, 1169 (2006).
[5] J. Z. Wu and Z. Li, Annu. Rev. Phys. Chem. **58**, 85 (2007).
[6] H. Löwen, J. Phys.: Condens. Matter **14**, 11897 (2002).
[7] W. G. Chapman, G. Jackson, and K. E. Gubbins, Mol. Phys. **65**, 1057 (1988).
[8] W. G. Chapman, K. E. Gubbins, G. Jackson, and M. Radosz, Fluid Phase Equilib. **52**, 31 (1989).
[9] M. S. Wertheim, J. Stat. Phys. **35**, 19 (1984).
[10] M. S. Wertheim, J. Stat. Phys. **35**, 35 (1984).
[11] M. S. Wertheim, J. Stat. Phys. **42**, 459 (1986).
[12] M. S. Wertheim, J. Stat. Phys. **42**, 477 (1986).
[13] A. GilVillegas, A. Galindo, P. J. Whitehead, S. J. Mills, G. Jackson, and A. N. Burgess, J. Chem. Phys. **106**, 4168 (1997).
[14] A. Galindo, L. A. Davies, A. Gil-Villegas, and G. Jackson, Mol. Phys. **93**, 241 (1998).
[15] F. J. Blas and L. F. Vega, Ind. Eng. Chem. Res. **37**, 660 (1998).
[16] J. C. Pamies and L. F. Vega, Ind. Eng. Chem. Res. **40**, 2532 (2001).
[17] J. Gross and G. Sadowski, Ind. Eng. Chem. Res. **40**, 1244 (2001).
[18] S. P. Tan, H. Adidharma, and M. Radosz, Ind. Eng. Chem. Res. **47**, 8063 (2008).
[19] C. J. Segura, W. G. Chapman, and K. P. Shukla, Mol. Phys. **90**, 759 (1997).
[20] C. J. Segura, E. V. Vakarin, W. G. Chapman, and M. F. Holovko, Mol. Phys. **108**, 4837 (1998).
[21] O. Pizio, A. Patrykiejew, and S. Sokolowski, J. Chem. Phys. **113**, 10761 (2000).
[22] F. J. Blas, E. M. del Rio, E. de Miguel, and G. Jackson, Mol. Phys. **99**, 1851 (2001).
[23] Y. X. Yu and J. Z. Wu, J. Chem. Phys. **116**, 7094 (2002).
[24] D. Fu and J. Z. Wu, Ind. Eng. Chem. Res. **44**, 1120 (2005).
[25] P. Bryk, S. Sokolowski, and O. Pizio, J. Chem. Phys. **125**, 024909 (2006).
[26] S. Tripathi and W. G. Chapman, J. Chem. Phys. **122**, 094506 (2005).
[27] S. Tripathi and W. G. Chapman, Phys. Rev. Lett. **94**, 087801 (2005).
[28] M. S. Wertheim, J. Chem. Phys. **87**, 7323 (1987).

[29] E. Kierlik and M. L. Rosinberg, J. Chem. Phys. **97**, 9222 (1992).
[30] E. Kierlik and M. L. Rosinberg, J. Chem. Phys. **99**, 3950 (1993).
[31] E. Kierlik and M. L. Rosinberg, J. Chem. Phys. **100**, 1716 (1994).
[32] M. Muller and L. G. MacDowell, Macromolecules **33**, 3902 (2000).
[33] Y. X. Yu and J. Z. Wu, J. Chem. Phys. **117**, 2368 (2002).
[34] A. Malijevsky, P. Bryk, and S. Sokolowski, Phys. Rev. E **72**, 032801 (2005).
[35] Y. Rosenfeld, Phys. Rev. Lett. **63**, 980 (1989).
[36] R. Roth, R. Evans, A. Lang, and G. Kahl, J. Phys.: Condens. Matter **14**, 12063 (2002).
[37] Y. X. Yu and J. Z. Wu, J. Chem. Phys. **117**, 10156 (2002).
[38] S. Phan, E. Kierlik, M. L. Rosinberg, B. Bildstein, and G. Kahl, Phys. Rev. E **48**, 618 (1993).
[39] S. Jain, A. Dominik, and W. G. Chapman, J. Chem. Phys. **127**, 244904 (2007).
[40] G. J. Gloor, F. J. Blas, E. M. del Rio, E. de Miguel, and G. Jackson, Fluid Phase Equilib. **194–197**, 521 (2002).
[41] G. J. Gloor, G. Jackson, F. J. Blas, E. M. del Rio, and E. de Miguel, J. Chem. Phys. **121**, 12740 (2004).
[42] G. J. Gloor, G. Jackson, F. J. Blas, E. M. del Rio, and E. de Miguel, J. Phys. Chem. C **111**, 15513 (2007).
[43] J. A. Barker and D. Henderson, J. Chem. Phys. **47**, 4714 (1967).
[44] J. Gross, AIChE J. **51**, 2556 (2005).
[45] J. Gross and J. Vrabec, AIChE J. **52**, 1194 (2006).
[46] J. Vrabec and J. Gross, J. Phys. Chem. B **112**, 51 (2008).
[47] M. Kleiner and J. Gross, AIChE J. **52**, 1951 (2006).
[48] A. Dominik, S. Tripathi, and W. G. Chapman, Ind. Eng. Chem. Res. **45**, 6785 (2006).
[49] J. Gross and G. Sadowski, Fluid Phase Equilib. **168**, 183 (2000).
[50] N. F. Carnahan and K. E. Starling, J. Chem. Phys. **51**, 635 (1969).
[51] S. Sokolowski and J. Fischer, J. Chem. Phys. **96**, 5441 (1992).
[52] Y. C. Chiew, Mol. Phys. **73**, 359 (1991).
[53] Y. Tang and B. C.-Y. Lu, J. Chem. Phys. **105**, 8262 (1996).
[54] J. Meunier, J. Phys. **48**, 1819 (1987).
[55] D. Bedeaux, in *Advances in Chemical Physics*, edited by I. Prigogine and S. A. Rice (Wiley, New York, 1986), Vol. 64.
[56] K. R. Mecke and S. Dietrich, Phys. Rev. E **59**, 6766 (1999).
[57] P. Tarazona, R. Checa, and E. Chacón, Phys. Rev. Lett. **99**, 196101 (2007).
[58] M. R. Moldover, Phys. Rev. A **31**, 1022 (1985).
[59] S. Fisk and B. Widom, J. Chem. Phys. **50**, 3219 (1969).
[60] H. Kahl and J. Winkelmann, Fluid Phase Equilib. **270**, 50 (2008).
[61] K. Binder, Phys. Rev. A **25**, 1699 (1982).
[62] E. Johannessen, J. Gross, and D. Bedeaux, J. Chem. Phys. **129**, 184703 (2008).
[63] The data for methane are taken from V. G. Baidakov, K. V. Khvostov, and G. N. Muratov, Zh. Fiz. Khim. **56**, 814 (1982); The data for ethane are from V. G. Baidakov and I. I. Sulla, Ukr. Fiz. Zh. (Russ. Ed.) **32**, 885 (1987); For all other n-alkanes, correlations provided by Ref. NIST, 2009 are here considered as quasiexperimental data.
[64] G. R. Somayajulu, Int. J. Thermophys. **9**, 559 (1988).
[65] E. W. Lemmon, M. O. McLinden, and D. G. Friend, NIST Standard Reference Database No. 69 (National Institute of Standards and Technology, Gaithersburg, MD, 20899, 2009), Chap Thermophysical Properties of Fluid Systems, http://webbook.nist.gov (retrieved August 17, 2009).
[66] C. C. Williams and B. J. Zwolinski, in *Selected Values of Properties of Hydrocarbons and Related Compounds* (American Petroleum Institute Research Project 44, Thermodynamic Research Center, Texas A&M University, College Station, 1980).
[67] J. J. Jasper, J. Phys. Chem. Ref. Data **1**, 841 (1972).
[68] S. Sugden, J. Chem. Soc. **125**, 32 (1924).
[69] P. Frodl and S. Dietrich, Phys. Rev. A **45**, 7330 (1992).
[70] P. Frodl and S. Dietrich, Phys. Rev. E **48**, 3741 (1993).
[71] P. Frodl, B. Groh, and S. Dietrich, Ber. Bunsenges. Phys. Chem **98**, 503 (1994).
[72] M. A. Osipov, P. I. C. Teixeira, and M. M. Telo da Gama, J. Phys. A **30**, 1953 (1997).
[73] M. Mecke, J. Fischer, and J. Winkelmann, J. Chem. Phys. **114**, 5842 (2001).
[74] S. Enders, H. Kahl, M. Mecke, and J. Winkelmann, J. Mol. Liquids **115**, 29 (2004).
[75] J. Winkelmann, J. Phys.: Condens. Matter **13**, 4739 (2001).
[76] N. B. Vargaftik, *Tables on the Thermophysical Properties of Liquids and Gases in Normal and Dissociated States*, 2nd ed. (Halsted, New York, 1975).
[77] G. N. Muratov and V. P. Skripov, Teplofiz. Vys. Temp. **20**, 596 (1982).